Molecular Biology of the Cell
Vol. 15, 3073–3082, July 2004

IRI-1, a LIN-15B Homologue, Interacts with Inositol-1,4,5-Triphosphate Receptors and Regulates Gonadogenesis, Defecation, and Pharyngeal Pumping in *Caenorhabditis elegans*

Denise S. Walker, Sung Ly, Nicholas J.D. Gower, and Howard A. Baylis*

Department of Zoology, University of Cambridge, Cambridge, CB2 3EJ, United Kingdom

Submitted January 16, 2004; Revised March 26, 2004; Accepted April 26, 2004
Monitoring Editor: Susan Strome

Inositol-1,4,5-triphosphate receptors (IP_3Rs) are ligand-gated Ca^{2+} channels that control Ca^{2+} release from intracellular stores. They are central to a wide range of cellular responses. IP_3Rs in *Caenorhabditis elegans* are encoded by a single gene, *itr-1*, and are widely expressed. Signaling through IP_3 and IP_3Rs is important in ovulation, control of the defecation cycle, modulation of pharyngeal pumping rate, and embryogenesis. To further elucidate the molecular basis of the diversity of IP_3R function, we used a yeast two-hybrid screen to search for proteins that interact with ITR-1. We identified an interaction between ITR-1 and IRI-1, a previously uncharacterized protein with homology to LIN-15B. *Iri-1* is widely expressed, and its expression overlaps significantly with that of *itr-1*. In agreement with this observation, *iri-1* functions in known *itr-1*–mediated processes, namely, upregulation of pharyngeal pumping in response to food and control of the defecation cycle. Knockdown of *iri-1* in an *itr-1* loss-of-function mutant potentiates some of these effects and sheds light on the signaling pathways that control pharyngeal pumping rate. Knockdown of *iri-1* expression also results in a sterile, *evl* phenotype, as a consequence of failures in early Z1/Z4 lineage divisions, such that gonadogenesis is severely disrupted.

INTRODUCTION

Intracellular signaling through inositol-1,4,5-trisphosphate (IP_3) is an important mechanism by which extracellular stimuli are transposed into changes in cellular physiology and gene expression (see Berridge, 1993, 1997; Clapham, 1995 for reviews). The only known activity of IP_3 is to regulate release of calcium through the IP_3 receptor (IP_3R). The widespread and multifunctional nature of calcium signals raises important questions as to the mechanisms that determine specificity, and a key determinant is likely to be through the modulation of the properties and spatial organization of calcium channels, such as IP_3Rs.

IP_3Rs are large tetrameric proteins located primarily in the ER (see Patel *et al.*, 1999, and Taylor *et al.*, 1999 for reviews). IP_3R subunits are proteins of ~2800 amino acids and are found in all animals analyzed to date. In mammals there are three subunit types, whereas *Caenorhabditis elegans* and *Drosophila* possess only one. All of these proteins share a common structure, with an amino-terminal domain of ~700 amino acids that is necessary and sufficient for binding IP_3, a carboxyl-terminal calcium channel domain consisting of six transmembrane regions and a large (~1400 residues) regulatory region between these two domains.

Many questions remain about the functions of IP_3Rs, particularly regarding the mechanisms by which IP_3 induced calcium signals are localized and regulated within cells to ensure the appropriate response to a given stimulus. It is clear that IP_3Rs are neither uniformly distributed within the ER, nor do they have uniform functional properties throughout the cell (see Taylor *et al.*, 1999 for review). Such diversity is likely to have important implications for the specificity of function. Clearly, interaction with other proteins is potentially an important determinant of both localization within a cell, and functional regulation. Therefore, with a view to elucidating the mechanisms responsible for specificity of IP_3 signaling, we have taken the approach of identifying protein interaction partners for IP_3Rs (Walker *et al.*, 2002b).

IP_3Rs in *C. elegans* are encoded by a single gene, *itr-1* and are widely expressed, in the nervous system, isthmus and terminal bulb of the pharynx, pharyngeo-intestinal valve, intestine, rectal epithelial cells, excretory cell, gonad sheath, spermatheca, uterine sheath, vulval hypodermis, and amphid socket cells (Baylis *et al.*, 1999; Dal Santo *et al.*, 1999; Gower *et al.*, 2001). Genetic studies have shown that *itr-1* is required for ovulation (Clandinin *et al.*, 1998) and the ultradian rhythm underlying defecation (Dal Santo *et al.*, 1999). Using a combination of a transgenic approach using an inducible IP_3 dominant-negative construct (IP_3 sponge), RNA interference and genetics we have shown that IP_3- and IP_3R-mediated signaling is required for the upregulation of pharyngeal pumping in response to food and that IP_3 signaling is required for multiple stages in embryogenesis (Walker *et al.*, 2002a). We have previously shown that at least one protein-protein interaction is required for the function of ITR-1 in the pharynx. ITR-1 interacts with myosin heavy chain II proteins, and transient disruption of this interaction in live animals interferes with the regulation of pharyngeal pumping (Walker *et al.*, 2002b). In this report we demonstrate that *C. elegans* IP_3Rs interact with IRI-1, a previously uncharacterized protein with homology to LIN-15B.

Article published online ahead of print. Mol. Biol. Cell 10.1091/mbc.E04–01–0039. Article and publication date are available at www.molbiolcell.org/cgi/doi/10.1091/mbc.E04–01–0039.
* Corresponding author. E-mail address: hab@mole.bio.cam.ac.uk.

ITR-1 and IRI-1 share many similarities in both expression pattern and function, suggesting that this interaction is important to the cellular function of IP_3Rs.

MATERIALS AND METHODS

Yeast Two-hybrid Analysis

A cDNA fragment encoding residues 1590–1951 of ITR-1 was amplified by PCR using Expand High Fidelity PCR System (Roche, Lewes, East Sussex, UK) and cloned in frame downstream of GAL4-AD in pAS2–1 (Harper *et al.*, 1993). This bait plasmid was used to screen a *C. elegans* cDNA library, which was kindly provided by R. Barstead, as described previously (Walker *et al.*, 2002b). Interactions were verified by retransformation of the isolated prey plasmid with the bait and with pAS2–1 (negative control), and assay of β galactosidase activity and the ability to grow in the absence of histidine. A cDNA fragment corresponding to amino acids 1276–1440 of LIN-15B (accession number U10412) was cloned in frame downstream of GAL4-BD in pACT2 (BD Clontech, Basingstoke Hampshire, United Kingdom) and tested in a similar way. Methods, vectors, and media were as described previously (Miguel-Aliaga *et al.*, 1999).

In Vitro Protein Interactions

A cDNA fragment encoding residues 734–867 of IRI-1 was amplified by PCR, with the addition of a consensus Kozak sequence (Kozak, 1986) and start codon. Following ligation into pGEM-T (Promega UK Ltd., Southampton, UK), the resulting plasmid was used to synthesize ^{35}S-labeled protein in the TNT coupled transcription/translation system (Promega). A cDNA fragment encoding residues 1590–1951 of ITR-1 was ligated into pGEX2T (Amersham Pharmacia Biotech, Little Chalfont, Buckinghamshire, United Kingdom). GST fusion protein purification and binding assays were performed as described previously, in TBS, 0.1% Triton X-100, using 500 nM fusion protein (Walker *et al.*, 1998).

C. elegans *Culture and Phenotypic Assays*

C. elegans strains were routinely cultured at 20°C on *Escherichia coli* OP50 grown on NGM plates (Brenner, 1974). Defecation and pharyngeal pumping were assayed at 20°C ~12 h after the onset of egg laying, as described previously (Walker *et al.*, 2002a). Pharyngeal pumping was analyzed by counting terminal bulb contractions, for 10 animals of each genotype, for 5 intervals of 30 s. The effects of serotonin were determined after incubation on NGM plus 7.5 mM hydroxytryptamine in the absence of food, for 1–2 h. Defecation cycles were analyzed by measuring the time interval between pBocs, for 10 animals of each genotype, for 10 cycles.

GFP Reporter Expression

A GFP reporter plasmid was constructed in pHAB200 (a derivative of pPD117.01; Baylis *et al.*, 1999). A PCR fragment of genomic DNA extending from 4 kb upstream to exon 2 of *iri-1* was translationally fused upstream of GFP, while a fragment extending from the stop codon to 2 kb downstream of *iri-1* was inserted downstream of GFP. The resulting plasmid was microinjected into *C. elegans* with the *rol-6* marker plasmid pRF4, and stable lines were examined for GFP expression pattern using a Leica SP laser scanning confocal microscope (Wetzlar, Germany). The *cnt-1A::gfp* reporter was constructed in pHAB200 in a similar way, using the *C. elegans* centaurin 1 gene. A genomic DNA fragment extending from 4 kb upstream to the end of exon 6 of the *cnt-1A* splice form was fused in frame upstream of *gfp*, and a fragment extending from the penultimate exon to 2 kb downstream was fused in frame downstream of *gfp* (L.S. Harrington and H.A. Baylis, unpublished data).

dsRNA-mediated Interference

For RNAi by feeding, base pairs 184-1575 of *iri-1* cDNA were ligated into pPD129.36, between the two convergent T7 polymerase promoters (Timmons *et al.*, 2001). Control plasmids were derivatives of pPD129.36 containing cDNA for GFP (pPD128.110; Timmons *et al.*, 2001) or chloramphenicol acetyl transferase (CAT). Plasmids were transformed into *E. coli* HT115 (DE3), and feeding was carried out as described previously (Walker *et al.*, 2002a), using the method of Timmons *et al.* (2001), except that bacterial lawns were grown at 37°C for 8 h. For RNAi from larval stage 1 (L1) onward, embryos were prepared by treatment of a plate containing many gravid adults with sodium hypochlorite (Lewis and Fleming, 1995). Embryos were incubated overnight in M9 buffer, allowing them to hatch but preventing development beyond L1. The resulting L1 preparation was then pipetted onto RNAi feeding plates. For RNAi by injection, base pairs 2200–2601 were ligated into pGEM-T (Promega), and the resulting plasmid was used as template for transcription from the T7 and SP6 promoters, using Megascript High Yield Transcription Kit (Ambion, Austin, TX), as described by the manufacturer. Following annealing of the two strands and isopropanol precipitation, dsRNA was injected into late L4 animals using standard procedures (Mello and Fire, 1995).

Statistical Analyses

The significance of differences between treatments was assessed using a modified Student's *t* test, where population variances are not assumed to be equal. Confidence intervals are either SEM or SD, as stated. For pharynx pumping and defecation interval, SD was calculated using all individual observations. Thus, for analysis of defecation, where, for each treatment, 10 animals were each observed for 10 defecation intervals, n = 100. Coefficient of variance (CV, SD expressed as a percentage of the mean) was calculated for individual animals, and these data were compiled to give mean CV for a given treatment.

RESULTS

An Interaction between ITR-1 and a Homologue of LIN-15B, Named IRI-1

To identify proteins that interact with IP_3 receptors, we used a yeast two-hybrid screen (Walker *et al.*, 2002b). IP_3 receptors are tetramers, and the subunits have three broadly defined regions, an N-terminal IP_3 binding domain of ~700 amino acids (see Baylis *et al.*, 1999 for evidence of this in ITR-1); a C-terminal domain that includes the membrane spanning regions and the channel pore that resides in the ER membrane; and, between these two regions, a large (~1400 amino acid) "regulatory domain" the function(s) of which are poorly understood (Figure 1A). Fragments of the *itr-1* cDNA corresponding to the regulatory domain were cloned into the bait plasmid, pAS2–1 and used to screen a *C. elegans* mixed stage random-primed cDNA library in pACT, kindly provided by R. Barstead.

When we used the region of *itr-1* corresponding to amino acids 1590–1951 (ITR-1 numbering is as in Baylis *et al.* (1999), EMBL accession number AJ243179) as bait we isolated a clone corresponding to the carboxyl terminal of a predicted protein, F44C4.4 (Figure 1B). We named this gene *iri-1*, for *I*P_3 *R*eceptor *I*nteracting protein.

IRI-1 and ITR-1 Interact In Vitro

To support the yeast two-hybrid–derived evidence that these two proteins interact, we determined whether peptides corresponding to the interacting regions could interact in vitro. As Figure 1C shows, a GST fusion protein containing residues 1590–1951 of ITR-1 interacts in vitro with residues 734–867 of IRI-1, translated in vitro in the presence of [^{35}S]methionine, whereas GST alone does not interact.

IRI-1 Is a Member of the LIN-15B Family

Figure 1B shows the gene structure of *iri-1*, based on our cDNA sequence, and Figure 1D shows the deduced amino acid sequence of the protein that it encodes (Genpep accession number: AAM48528). IRI-1 shows homology to LIN-15B, a negative regulator of ectopic vulval induction (Clark *et al.*, 1994; Huang *et al.*, 1994), which has also recently been identified as a negative regulator of progression into G1 of the cell cycle (Boxem and van den Heuvel, 2002). LIN-15B is the founding member of a family of *C. elegans* predicted proteins, for which homologues have not as yet been identified in other organisms. The degree of homology is relatively low overall (e.g., IRI-1 and LIN-15B share only 13% identity, 45% conservation overall), but they share discrete blocks of more substantial homology (Figure 2A). In addition, most members of this family are predicted to have a carboxyl-terminal proline-rich domain, the length of which varies considerably. As Figure 1D shows, the region of IRI-1 identified as interacting with ITR-1 maps to this proline-rich domain.

Because LIN-15B is the closest homologue of IRI-1, we determined whether the interaction with ITR-1 is conserved in LIN-15B, using the yeast two-hybrid system. A cDNA

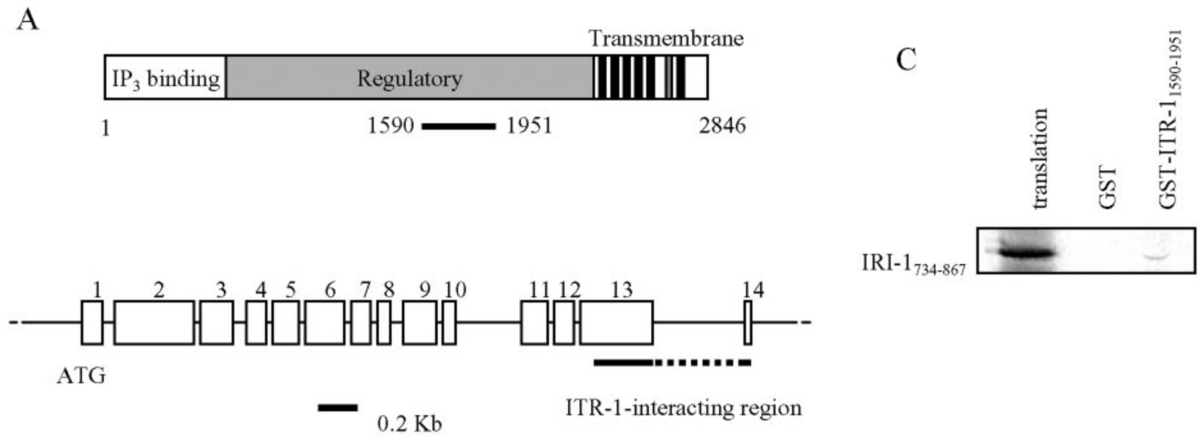

D

MVIVPKDPENLKNWMEKYDFQIKTIMAGSVHFLCKTHLSEDKSVERIPSSSVESATEQYM 60
LEIKEEEPYSQAGSSSESWPEVKEEVIEPVEEIDYDHMPFEIEQNSYETFDESKSYHNSY 120
ESDHHQPTTSTSATRAIRRPTTKSLEFTNLPTYLQELSDGEILSFCVKTSSNLSGATSLE 180
CGMCEEQYFNSTDTRPIRHHLISRHEATMKKYKNHFPITAAPKIYAPIQQVTIDRADQAL 240
TKFFIKSGIPLRAVQDRNLNMLAFNMNSEYSLPTVETMHSFLEKIADAKANAKLNFDDSP 300
VTITFDTTTFNNRHYLAFTVHYYHIRSRMRRCIFLREYDMTGPIVPSVMTAIQKTIEESG 360
SRLKITTVVAGKAEFEDALEDMHSFKQVMICFSQNINKFAETLIEHPVFAGPLQKLRDFI 420
TKFPTHRNSWGKFKSYIVKKRTYGEYPEVDNGHWITTLDFITKCLHMHRLFSEFVSTSAQ 480
LQYIDVEDNVNIVYLHSLLNLCKSALKEMVDVKATIADVIPAIADISFSLIVTTSKQTVV 540
DAVSTIFNQLLLPFVEQSDIHRFALFLHPLRHGSDLLASADWMKIKTDLSSHLSLREAAE 600
ATLAHPSSFDNTITADKEVNAFSQYVCRVTGVETGIMDWWARHAGRFPRLYKYARELFII 660
PAFSIDAAYYLGEYGILTHSINESDISKRKMLLRAASELVEYRSKGSLMCKPICVKRRKD 720
ANSPEDAWYHAIDVRALQIVDVPS**DEPPKRMIPQRTPFVYQNPNPLPPHRILQSFPT**IRT 780
NREAPHGRSLKDEIAKIAANRQKIQRVYTVASSSPYARPVVVKTESKEGIVEQLTPSAPP 840
PKRYYAVRPAAGNGTSVIRGKDESPST* 867

Figure 1. IRI-1, a previously uncharacterized protein, interacts with the regulatory domain of the ITR-1. (A) Schematic diagram of ITR-1, showing IP_3 binding, regulatory, and transmembrane domains. Bar below indicates the region identified as interacting with IRI-1. (B) Gene structure of *iri-1*, based on cDNA sequence. Boxes represent exons. Bar below indicates the region identified in a yeast two-hybrid screen as encoding a peptide that interacts with ITR-1. (C) In vitro binding of ^{35}S-IRI-$1_{734-867}$ with a GST-ITR-$1_{1590-1951}$ fusion protein. (D) Amino acid sequence of IRI-1. ITR-1–interacting sequence is underlined (solid line). Overlapping pat 4 and pat 7 consensus sequences are underlined (dotted line). The region showing structural similarity to a region of RanGAP1, and sequence similarity to cytocentrin and RalBP1, is shown in bold.

fragment corresponding to the carboxyl-terminal 165 amino acids of LIN-15B (which, by alignment, correspond most closely to the ITR-1 interacting region of IRI-1) was ligated into pACT2 (Clontech) and tested for interaction with the bait plasmid, a derivative of pAS2–1 containing a cDNA fragment encoding residues 1590–1951 of *itr-1*. As Figure 2B shows, this region of ITR-1 clearly interacts with amino acids 734–867 of IRI-1, but not the corresponding region of LIN-15B.

The lack of homology with known functional motifs or domains makes it difficult to make predictions about the cellular basis of IRI-1 function. Amino acids 745–778 are predicted (using SMART; Schultz *et al.*, 1998; Letunic *et al.*, 2002) to be structurally similar to an alpha-alpha superhelix found in Ran GTPase activating protein 1 (RanGAP1), a cytosolic protein involved in nucleocytoplasmic transport (Nishimoto, 2000). The most significant primary sequence homology with non-*C. elegans* proteins involves the same region. It shares homology with the closely related GAPs cytocentrin, which regulates mitotic spindle assembly (Quaroni and Paul, 1999) and RalBP1, a GAP for CDC42 and Rac, which regulate the actin cytoskeleton (Ridley, 1995). In both cases, though, the relevant regions of these proteins are of unknown function. Analysis of the primary sequence of IRI-1 (using PSORT II; Nakai and Horton, 1999) indicates the presence of a putative transmembrane domain (residues 516–534) and potential nuclear discrimination signals (pat4, KRRK, starting at residue 716, and pat7, PICVKRR, starting at residue 712). However, in common with RabGAP1 (Matunis *et al.*, 1998) there are also 11 motifs that bear a resemblance to leucine-rich nuclear export signals ($\psi X_{n\psi} X_{2\psi} X \psi$, where ψ is hydrophobic), suggesting that IRI-1 could shuttle between the nucleus and cytoplasm. Proline-rich domains are important in a wide range of protein-protein interactions, particularly among signaling proteins (Kay *et al.*, 2000 for review), and indeed the carboxyl terminal region of IRI-1 contains two potential PXXP motifs, similar to those known to bind SRC homology 3 (SH3) domains.

IRI-1 Is Widely Coexpressed with ITR-1

If the interaction between IRI-1 and ITR-1 has functional significance, we would expect them to be to be expressed in the same cells. To determine where IRI-1 was expressed, we constructed a reporter plasmid encompassing 4 kb upstream and 2 kb downstream of *iri-1*, with GFP fused to the second exon of *iri-1*. As Figure 3 shows, the *iri-1::gfp* expression

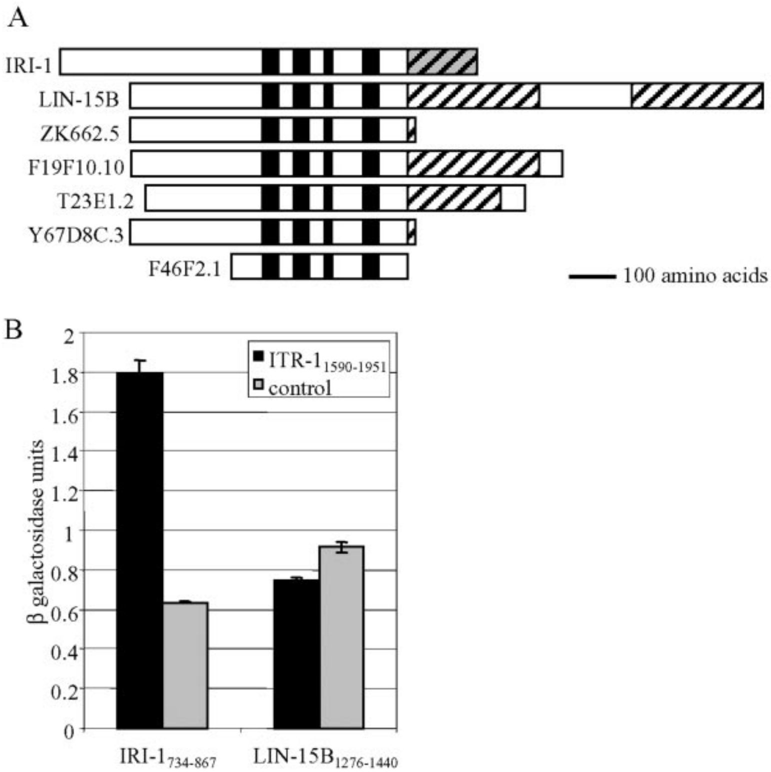

Figure 2. IRI-1 is a member of a LIN-15B-like family of *C. elegans* proteins. (A) Schematic representation of an alignment of *C. elegans* proteins and predicted proteins displaying homology to LIN-15B. Black boxes are regions of more significant sequence conservation. Hatched boxes are proline-rich regions. Shaded box indicates the region of IRI-1 that interacts with ITR-1. (B) Yeast two-hybrid assay to show that ITR-$1_{1590-1951}$ interacts with IRI-$1_{734-867}$, but not with the corresponding region of LIN-15B. *Iri-1* and *lin-15B* fragments were cloned into pACT2, and the *itr-1* fragment was cloned into pAS2–1. These were transformed into *S. cerevisiae* PJ69-4A and interactions assayed by measuring β-galactosidase activity. Control indicates pAS2–1 lacking the *itr-1* insert. Mean activity from three separate assays. Error bars are SEM.

pattern shares many similarities with *itr-1* (Baylis *et al.*, 1999, Dal Santo *et al.*, 1999, Gower *et al.*, 2001). Both are expressed in the terminal bulb of the pharynx, amphid socket cells, pharyngeal-intestinal valve, intestine, excretory cell, rectal epithelial cells, and vulva hypodermis. In addition, *iri-1::gfp* is expressed in the corpus of the pharynx, the pharyngeal neuron I3, the anal sphincter and in the gonad precursor cells Z1 and Z4.

IRI-1 Functions in Pharyngeal Pumping and Defecation

To unravel the potential function of the ITR-1–IRI-1 interaction, we knocked down *iri-1* expression by RNA-mediated interference (RNAi). Two different cDNA fragments of *iri-1*, corresponding to amino acids 115–525 and 734–867, were used in RNAi by feeding and injection, respectively.

Because ITR-1 functions in the upregulation of pharyngeal pumping in response to food (Walker *et al.*, 2002a), we tested whether IRI-1 also functions in pharyngeal pumping. As Figure 4A shows, RNAi by feeding and injection both result in a significant decrease (39.4 and 37.1%, respectively, $p < 0.001$ in each case) in the rate of pharyngeal pumping in the presence of food, whereas basal pumping rate is unaffected. In addition, knockdown of *iri-1* expression also increased the variability of pumping rate in response to food, as we have previously observed for disruption of *itr-1* function (Walker *et al.*, 2002a). For example, for *iri-1* RNAi by feeding the mean CV was 13.13 ± 8.83, compared with 4.95 ± 1.48 for *gfp* RNAi by feeding (error intervals are SD, $p < 0.05$). We therefore tested the effect of exogenous application of serotonin, which mimics the effect of food, causing upregulation of pumping rate in wild-type animals. The response to serotonin is unaltered by knockdown of IRI-1 expression (Figure 4A). Thus the pharyngeal muscle is still able to respond to serotonin and pump at a significantly higher rate (compared with pumping in the absence of food, $p < 0.001$). We conclude that IRI-1 functions in the upregulation of pumping in response to food, an IP_3-mediated process.

Defecation is a regular, rhythmic process that consists of three coordinated muscle contractions: posterior body wall muscle contraction (pBoc), anterior body wall muscle contraction (aBoc), and enteric muscle contraction (EMC), resulting in expulsion of intestinal contents (Liu and Thomas, 1994). ITR-1 functions in the control of the defecation cycle (Iwasaki *et al.*, 1995), via generation of an intestinal calcium transient before pBoc (Dal Santo *et al.*, 1998). Interference with IP_3 signaling or *itr-1* expression results in not only a significant increase in the mean length of the defecation cycle, but also a dramatic increase in the variability of cycle length, and in some cases a complete failure of animals to defecate (Walker *et al.*, 2002a). We therefore tested whether IRI-1 also functions in this ITR-1–mediated process. As Figure 4B shows, the effect on defecation cycle interval is distinct from that observed after disruption of ITR-1 function, in that although the mean cycle length increases only slightly (but significantly, $p < 0.001$ for both feeding and injection), the same dramatic increase in variability of cycle length is observed. For example, for *iri-1* RNAi by feeding, the mean coefficient of variance is 30.10 ± 30.77, compared with 12.70 ± 8.22 for *gfp* (this difference is not statistically significant, because of the fact that between-worm variation is also extensive. For comparison, *itr-1* (*sa73*) animals exhibited a mean coefficient of variance of 27.53 ± 16.62 when assayed in the same way, error intervals are SD). In addition, a significant proportion of EMCs are missed ($p < 0.01$ for both feeding and injection), particularly as a result of *iri-1* RNAi by feeding (Figure 4C). Mutations that affect both cycle timing and the execution of muscle contractions are rare, suggesting a functional separation between these two aspects of defecation. However, mutations in *flr-1*, which is only expressed in the intestine, result in both shorter cycles

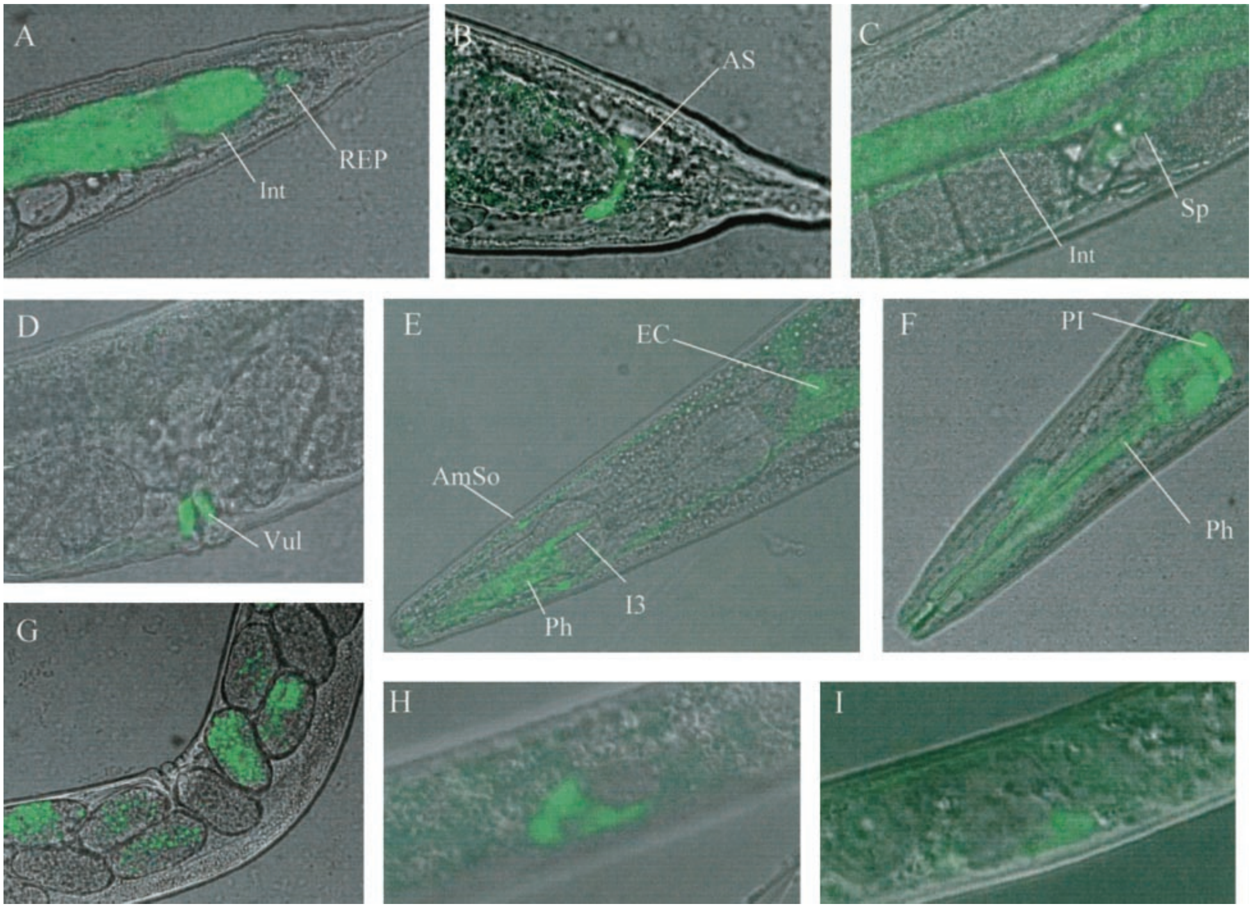

Figure 3. *Iri-1* is widely expressed. (A–H) An *iri-1::gfp* fusion is expressed in the intestine (Int; A and C), rectal epithelial cells (REP; A), anal sphincter (AS; B), spermatheca (Sp; C), vulval hypodermis cells (Vul; D), excretory cell (EC; E), amphid socket cells (AmSo; E), the pharyngeal neuron I3 (E), procorpus, corpus, isthmus, and terminal bulb muscles of the pharynx (Ph; E and F), and the pharyngeo-intestinal valve (PI; F). It is widely expressed in developing embryos (G) and is expressed in the gonad precursors Z1 (H) and Z4 (I). Maximal projections of serial z-sections of GFP fluorescence, overlaid with a single midsection transmission image.

and EMC failure (Takeuchi *et al.,* 1998), indicating that defects in EMC can result from failures in the signaling mechanisms that control timing. With respect to *iri-1* knockdown, the length of cycles preceding EMC failure was not significantly shorter ($p > 0.05$), suggesting that this is unlikely to be the explanation. We conclude that IRI-1 functions not only in the control of defecation cycle length, an ITR-1 mediated process, but also in EMC.

Functional Interaction between ITR-1 and IRI-1

To establish whether there is a functional relationship between ITR-1 and IRI-1 in upregulation of pharynx pumping, we examined the effects of knocking down *iri-1* expression in the reduction-of-function mutant *itr-1* (*sa73*) (Iwasaki *et al.,* 1995). As Figure 5A shows, untreated *itr-1* (*sa73*) mutants exhibit a reduced rate of pharyngeal pumping in the presence of food (Walker *et al.,* 2002a). Treatment with exogenous serotonin results in significant upregulation of pumping rate, compared with that in the absence of food. Knocking down *iri-1* expression (by RNAi by feeding) in *itr-1 (sa73)* results in a reduction of pumping rate, in the presence of food, that is not significantly different ($p > 0.05$) from those seen for untreated *itr-1* (*sa73*) animals and for *iri-1* RNAi by feeding of wild-type animals (157.72 ± 33.86 vs. 155.04 ± 23.38 and 140.12 ± 61.59, respectively, error intervals are SD), indicating an absence of any synergistic effect. By contrast, *iri-1* RNAi treatment of *itr-1* (*sa73*) animals significantly disrupts the response to exogenous serotonin, such that serotonin only slightly (but significantly, $p < 0.01$) increases pumping rate compared with that observed in its absence (i.e., "off food"). The upregulation of pumping in response to serotonin (compared with "no food") is significantly smaller than for *itr-1* (*sa73*) or *iri-1* (*RNAi*) or control animals; the actual rate of pumping on serotonin plates is also significantly lower than for any of the other treatments ($p < 0.001$ in all cases). Indeed, the pumping rate in response to exogenous serotonin is significantly lower than that observed in response to food ($p < 0.001$). Because *iri-1* (*RNAi*) has no effect on upregulation of pumping rate in the presence of serotonin and *iri-1* (*RNAi*) in an *itr-1* (*sa73*) background has significantly greater effect than *itr-1* (*sa73*) alone, we conclude that reducing the function of the two genes is synergistic in the response to exogenous serotonin.

Similarly, we examined the effect of *iri-1* knockdown in *itr-1* (*sa73*) animals on regulation of the defecation cycle. As Figure 5B shows, the defecation cycle in untreated *itr-1* (*sa73*) animals is significantly longer than in wild-type animals, as reported previously (Dal Santo *et al.,* 1999). When *itr-1* (*sa73*) animals are treated with *iri-1* RNAi, the defeca-

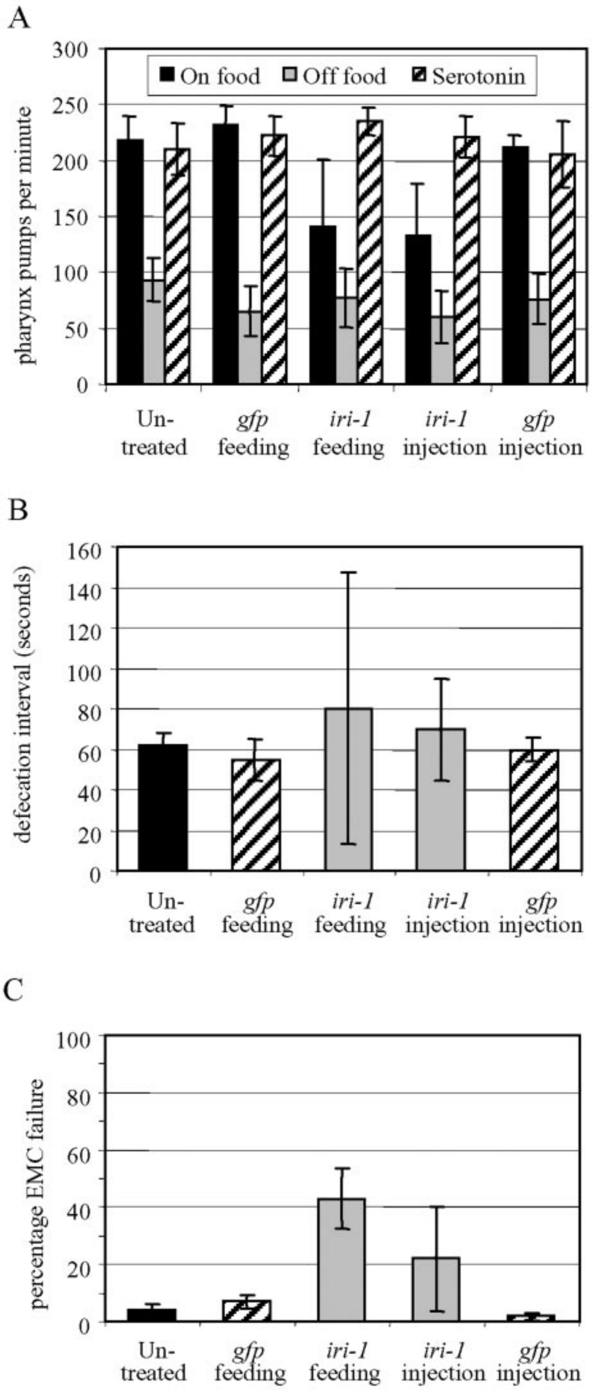

Figure 4. *Iri-1* functions in the control of pharyngeal pumping rate and defecation. (A) Mean pharyngeal pumping rate, after RNAi by feeding or injection, of *gfp* (control) or *iri-1*. Error bars, SD; n = 50 for each treatment. (B) Mean defecation cycle length of RNAi treated animals. Error bars, SD; n = 100 for each treatment. (C) Mean percentage of enteric muscle contractions that were not correctly performed, from the results for individual animals that were observed for B. Error bars, SEM; n = 10 for each treatment.

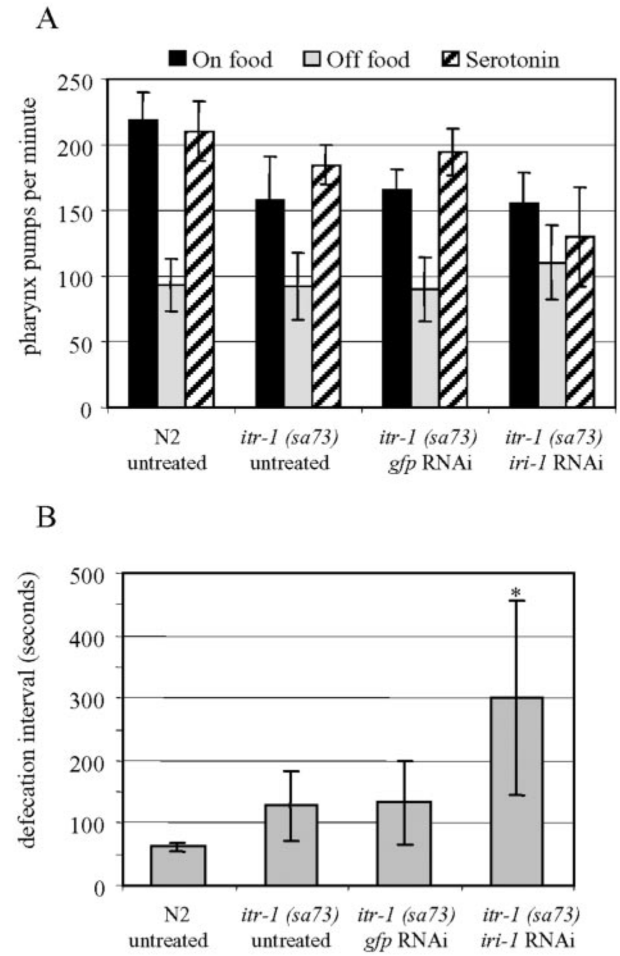

Figure 5. Functional interaction between *iri-1* and *itr-1*. (A) Mean pharyngeal pumping rate of *itr-1* (*sa73*) animals (and N2 for comparison), after RNAi by feeding of *gfp* (control) or *iri-1*. Error bars, SD; n = 50 for each treatment. (B) Mean defecation cycle length of RNAi treated animals. Error bars, SD, n = 100 for each treatment, except: * 70% of *iri-1* RNAi-treated *itr-1 (sa73)* animals exhibited cycle lengths greater than 10 min and are therefore excluded from the mean (thus n = 30).

tion cycle is much more substantially disrupted than for either untreated *itr-1* (*sa73*) or for *iri-1* RNAi-treated N2 animals. Indeed the results shown in Figure 5B severely underestimate the effects, because 70% of animals failed to defecate within 10 min, and these results are excluded from the mean. This is analogous to the effects that we observed after severe disruption of *itr-1* function by, for example, overexpression of an IP_3 sponge or by RNA interference of *itr-1* (Walker *et al.*, 2002a). In addition, *iri-1* knockdown on *itr-1* (*sa73*) animals results in a substantial decrease in growth rate, which is more substantial than that observed for untreated *itr-1 (sa73)* animals. Compared with untreated N2 or *iri-1* RNAi-treated N2, untreated *itr-1* (*sa73*) animals take ~24 h longer to reach adulthood, as reported previously (Dal Santo *et al.*, 1999), whereas *iri-1* RNAi–treated *itr-1* (*sa73*) animals take ~48 h longer, at 20°C.

IRI-1 Functions in Z1 and Z4 Lineages in Early Gonadogenesis

The most visually striking consequence of *iri-1* knockdown (observed in 50% of animals) is a malformation of the vulva (Figure 6A), which may be analogous to phenotypes observed in *pvl* (protruding vulva; Eisenmann and Kim, 2000; Friedman *et al.*, 2000) or *evl* (abnormal eversion of the vulva;

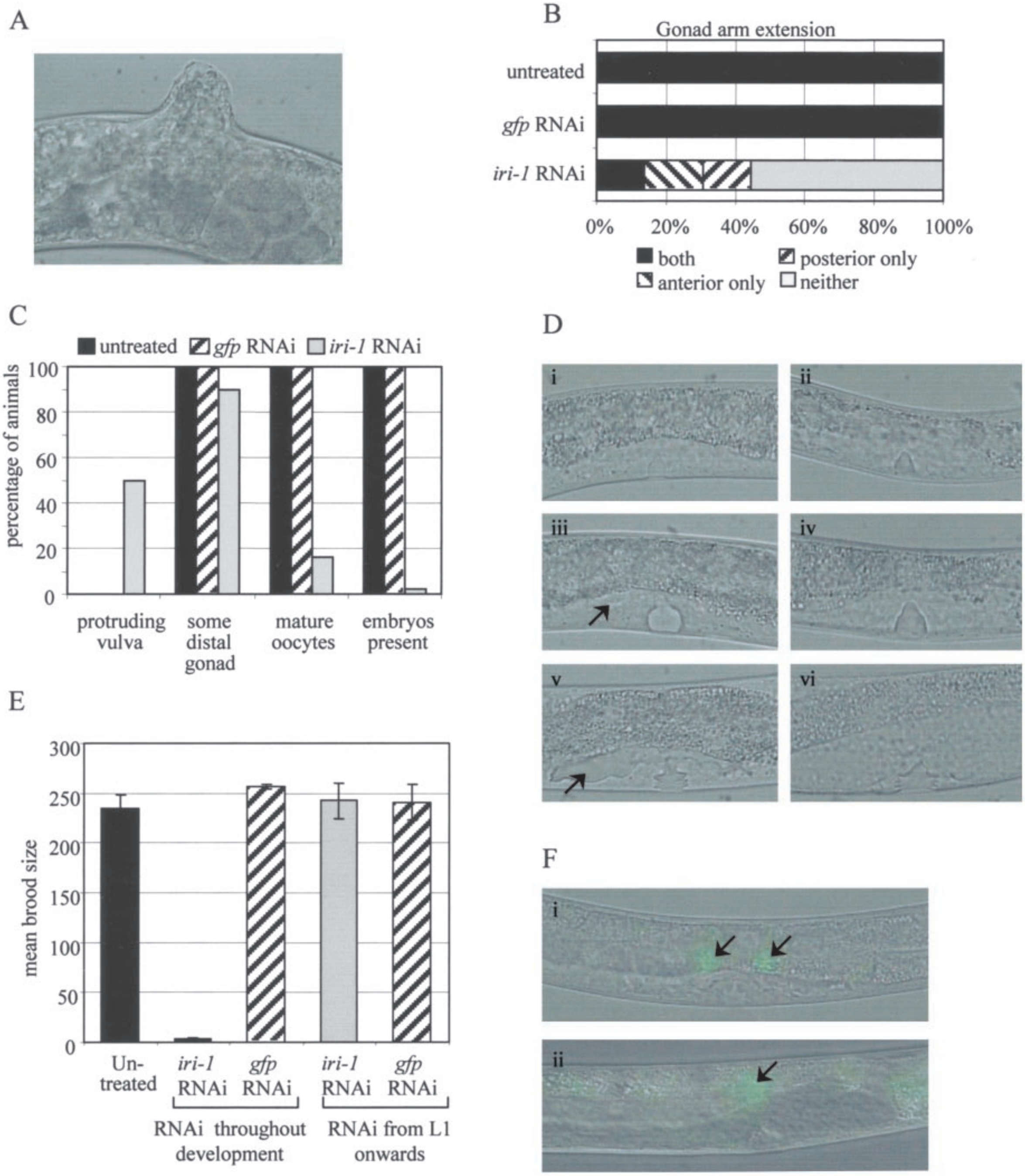

Figure 6. Knockdown of *iri-1* expression severely disrupts gonadogenesis. All data for this figure was compiled using RNAi by feeding. RNAi by injection gave similar results. (A) Nomarski image of the protruding vulva phenotype resulting from knockdown of *iri-1* expression. (B) Percentage of RNAi-treated animals showing some degree of (but not necessarily complete) gonad extension (n = 36 for each treatment). (C) Percentage of RNAi treated animals exhibiting the gonadal characteristics indicated (n = 44 for each treatment). (D) Nomarski micrographs showing successive stages of vulva morphogenesis from invagination of vulval precursors during larval stage 3 (i and iv) to "Christmas tree" stage during larval stage 4 (v and vi). RNAi of *gfp* (i–iii) and of *iri-1* (iv–vi). Arrows indicate uterine cavity. (E) Mean brood size of animals treated with RNAi by feeding either throughout development (standard protocol) or from larval stage 1 onwards only. Error bars, SEM; n = 7 for each treatment. (F) L4 larvae transgenically expressing *cnt-1A::gfp* to label distal tip cells. (i) *Cat* RNAi (control) animals exhibited proper extension and turning of both gonad arms, and *cnt-1A::gfp* expression in both DTCs (arrows). (ii) A common phenotype for *iri-1* RNAi animals was that one gonad arm extended and turned correctly and showed *cnt-1A::gfp* expression in the DTC (arrow), while the other arm failed to extend and did not possess a DTC.

Seydoux *et al.*, 1993) mutants. In addition, the vast majority of animals (98%) are sterile as a result of severely malformed gonads. Although a germline can be detected, most animals fail to properly extend gonad arms and do not have a detectable spermatheca or uterus, such that they fail to produce mature oocytes and thus embryos (Figure 6, B and C).

Vulva development in *C. elegans* consists of several distinct stages; "generation," in which the blast cells that will give rise to the vulva are born; "fate specification," in which extracellular signals determine the fates of these cells; "execution," in which these divide and differentiate to generate 22 vulval cells; and "morphogenesis," in which they undergo extensive morphogenetic movements culminating in eversion to form the opening connecting the uterus with the exterior (Ferguson *et al.,* 1987; Greenwald, 1997). Defects in vulva eversion can occur not only as a direct result of defective vulva morphogenesis, but also as an indirect result of defective development of the somatic gonad, because anchoring of the vulva relies on the integrity of the uterus (Seydoux *et al.,* 1993). Given that knockdown of *iri-1* expression severely disrupts somatic gonad development, we examined whether it affects vulva morphogenesis before eversion. As Figure 6D shows, in late L3 animals the vulval precursor cells (VPCs) invaginate. This invagination changes shape as it grows, resulting in the characteristic "Christmas tree" shape at mid-late L4 stage. The sides of the invagination then meet in the center and evert to form the lips of the mature vulva. *Iri-1* knockdown does not produce any detectable effect on the stages leading up to eversion, suggesting that the phenotype observed is indeed an indirect result of defective uterine development. In agreement with this hypothesis, although *iri-1::gfp* is expressed in the hypodermis of the mature vulva, no expression is detected until after the completion of vulva morphogenesis.

The severe disruption of gonadogenesis observed following *iri-1* RNAi suggests a role in the earlier stages of gonad formation. In agreement with this idea, deficiencies that result in analogous end phenotypes (e.g., *pop-1*, *sys-1*, *gon-4*, as discussed later) have been shown to disrupt the early lineages that eventually give rise to the somatic gonad. The similarities with the phenotype resulting from *iri-1* knockdown lead us to hypothesize that IRI-1 functions early in the Z1/Z4 lineages, which coincides well with the expression of *iri-1::gfp* in Z1 and Z4 (Figure 3, H and I).

To support our hypothesis that the function of *iri-1* in gonadogenesis is in the very early Z1/Z4 lineage cell divisions and that it does not function later, we examined the effect of knocking down *iri-1* expression only after the first larval stage. As Figure 6E shows, *iri-1* RNAi had no significant effect on brood size when animals were treated only after the first larval stage, supporting our hypothesis that the sterility resulting from knockdown of *iri-1* expression originates from disruption of *iri-1* function in Z1 and Z4. In contrast, RNAi treatment in this way significantly disrupted other functions associated with *iri-1* (e.g., pharynx pumping rate after *iri-1* RNAi by feeding was 153.68 ± 32.58, compared with 214.32 ± 14.55 for *gfp* RNAi, $n = 25$ for each treatment, $p < 0.001$, error intervals are SD), indicating that this approach can effectively disrupt *iri-1* function and, furthermore, that the effect on pharynx pumping is not due to an early developmental defect.

Z1 and Z4 give rise to two distal tip cells (DTCs), one at the end of each germ line tube. These stimulate germ line growth and act as "leaders," directing the extension of the growing gonad arms. Indeed, in the absence of DTCs, the germ line consists of only a few sperm and the gonad arms fail to extend (Kimble and White, 1981). To examine the role of DTCs in the generation of the phenotype observed, we carried out RNAi by feeding on a strain expressing a GFP marker for DTCs, *cnt-1A::gfp* (L.S. Harrington and H.A. Baylis, unpublished data, see MATERIALS AND METHODS for a description). One hundred percent of control treated animals exhibited expression of *cnt-1::gfp* in both of their DTCs. In contrast, only 33% of *iri-1* RNAi animals possessed two DTCs, expressing *cnt-1::gfp*, whereas 50% had only one and 17% had neither (Figure 6F). A strong correlation was observed in *iri-1* RNAi animals, between the degree of arm extension and the presence of DTCs. Ninety-six percent of gonad arms lacking a DTC failed to extend, whereas, of those that did possess a DTC, 77.1% extended normally and 8.6% extended partially. The remaining 14.3% failed to extend and exhibited defective, rounded DTCs ($n = 30$ for each treatment).

More detailed analysis of the Z1/Z4 lineages revealed that early divisions were randomly aborted. The extent to which divisions occurred varied considerably between animals, but also within animals. Indeed, in many animals, while one of the lineages was severely compromised, the other continued normally (unpublished data).

DISCUSSION

We have identified a direct interaction between the *C. elegans* IP_3 receptor, ITR-1, and a LIN-15B homologue, IRI-1. IRI-1 plays a role in key physiological processes mediated by IP_3 signaling, suggesting that the interaction also plays a significant role in these processes. However, both proteins also play roles in processes in which the other is not implicated.

IRI-1 and Modulation of Pharyngeal Pumping Rate

C. elegans responds to the presence of food by making adaptive changes in several behavioral processes, including locomotion, egg laying, defecation, and pharyngeal pumping. The pharynx is a neuromuscular organ that contracts and relaxes rhythmically to ingest food and transport it posteriorly into the intestine. The rate of contraction increases in response to the presence of food and decreases when food is scarce. Exogenous serotonin mimics the effect of food, increasing pumping rate, whereas octopamine has the opposite effect (Horvitz *et al.,* 1982; Avery and Horvitz, 1990). These effects are dependent on the action of the pharyngeal motor neurons MC and M3, which trigger and terminate muscle action potentials, respectively. Serotonin acts to increase the activity or effect of both these neurons, thereby decreasing action potential duration, although it is unclear as yet whether the site of action is the neurons themselves or the muscle (Niacaris and Avery, 2003).

We have shown that the upregulation of pharyngeal pumping in response to food is dependant on intact IP_3- and IP_3R-mediated signaling (Walker *et al.,* 2002a). Disruption of IP_3 signaling or ITR-1 function does not ablate the upregulation of pharynx pumping in response to serotonin (Walker *et al.,* 2002a), indicating that muscle function per se is not compromised. Our data indicate that, in common with ITR-1, IRI-1 is expressed in the isthmus and terminal bulb as well as being expressed in the other pharyngeal muscles and in I3, a pharyngeal interneuron whose function remains unclear. We have demonstrated that the effect of knockdown of *iri-1* is similar to that of disrupting IP_3 signaling or ITR-1 function, in that pumping rate on food is reduced but the ability to upregulate pumping rate in response to exogenous serotonin is unaffected. This similarity, coupled with the coexpression of IRI-1 and ITR-1 in the isthmus and terminal bulb, and the demonstration that the two proteins interact, led us to investigate their functional relationship in the pharynx in more detail. To this end, we examined the effect of *iri-1* RNAi in the mild loss-of-function mutant *itr-1* (*sa73*; Iwasaki *et al.,* 1995). The pharyngeal pumping rate of *itr-1* (*sa73*) on food is not significantly altered by *iri-1* RNAi, perhaps suggesting that *itr-1* and *iri-1* are closely associated in the same signaling pathway controlling the response to food. Interestingly though, in contrast to either untreated *itr-1* (*sa73*) or *iri-1* RNAi of wild-type animals, *iri-1* RNAi of *itr-1* (*sa73*) animals severely disrupts the response to exogenous serotonin, such that the pumping rate in these conditions is barely greater than that observed in the absence of food. One explanation for this would be that *itr-1* and *iri-1* function in the same pathway and that upregulation in response to serotonin requires a threshold level of a given component of the signaling pathway. If *itr-1* (*sa73*) or *iri-1* (*RNAi*) does not exert sufficient effect alone, this threshold will still be reached, whereas the combination of *itr-1* (*sa73*) and *iri-1* (*RNAi*) would have a greater impact on *itr-1*–mediated signaling, such that this threshold is no longer reached. This hypothesis fits well with our previous observation that more severe disruption of *itr-1* function, using RNAi, also disrupts the response to serotonin (Walker *et al.,* 2002a). The fact that neither approach completely disrupts upregulation in response to serotonin suggests that an *itr-1*–independent pathway is also involved. Meanwhile, the clear distinction between the effects on the response to food and the response to exogenous serotonin indicates a distinction in the signaling pathways responsible, in which the role of *itr-1*–mediated signaling merits further investigation. In the present study, for example, we have investigated only one allele of *itr-1*, and investigation of others could shed new light on the role of *itr-1*. The fact that *iri-1* and *itr-1* are both expressed in the isthmus and terminal bulb suggests that one of these is the site of action for both proteins, with respect to their roles in modulation of pumping rate and that this is where the interaction is significant. *Iri-1* is more widely expressed in the pharynx, however, and although we have good evidence that IRI-1 and ITR-1 can interact in vitro, it is unclear as yet whether this interaction is functionally significant in vivo, so the functional relationship may well be far more complex.

IRI-1 and Control of Defecation

Defecation, like pharyngeal pumping, represents a valuable model system in which to investigate the roles of IP_3 signaling in the generation of endogenous rhythms. We have demonstrated that knockdown of *iri-1* expression results in a subtle increase in mean defecation interval, a dramatic increase in the variability of cycle length, and a significant failure of EMC. The first two of these coincide well with the role of IP_3Rs in defecation, although disruption of IP_3R-mediated signaling has a more substantial effect on cycle length. EMC consists of the coordinated contraction of the anal depressor, intestinal and anal sphincter muscles, so this fits well with our observation that *iri-1*, unlike *itr-1*, is expressed in the anal sphincter.

Knocking down *iri-1* expression appears to potentiate the effect of the *itr-1* (*sa73*) mutation on defecation, such that the defecation rhythm is almost completely disrupted, as in animals carrying the more severe allele, *itr-1* (*n2559*) or *itr-1* RNAi animals (Dal Santo *et al.,* 1999; Walker *et al.,* 2002a). This suggests that the combined effect of the *itr-1* (*sa73*) mutation and *iri-1* knockdown almost completely disrupts *itr-1* function in defecation. *Itr-1* appears to control defecation cycle length via the production of an intestinal calcium wave before the initiation of pBoc (Dal Santo *et al.,* 1999). It is interesting in this respect that *iri-1* is also expressed in the intestine, suggesting that this is where the interaction is functionally significant.

IRI-1 and Gonadogenesis

Knockdown of *iri-1* expression by RNAi results in severe disruption of gonadogenesis, such that most somatic gonad structures do not form and gonad arms fail to extend. As a result of the absence of the uterine cells required for attachment, the vulva often everts abnormally. *Iri-1* is expressed in the somatic gonad precursors, Z1 and Z4, and we have shown that *iri-1* functions in early Z1/Z4 lineage cell divisions. The observed phenotype coincides well with the phenotypes described for mutants that affect these early divisions. Mutations affecting members of a Wnt signaling pathway, such as *pop-1* (Siegfried and Kimble, 2002) and *sys-1* (Miskowski *et al.,* 2001) result in symmetrical divisions in the Z1/Z4 lineages, with the result that DTCs are absent. The somatic gonad precursors fail to cluster to form the gonad primordium, resulting in a high incidence of *pvl*, and failure of gonad arms to extend. In *gon-4* mutants (Friedman *et al.,* 2000), Z1/Z4 lineages are variably aborted, with the result that normal somatic gonad structures are never observed and either one or no DTCs are present, and there is a high incidence of *pvl*, but also *muv* (multiple vulva) and *vul* (vulvaless). As one would expect, a clear correlation was observed between the presence (and correct morphology) of DTCs and the ability of gonad arms to extend. An asymmetry was common, such that in many cases only one arm extended, correlating with the presence of a single DTC.

Genetic evidence indicates that *itr-1* functions downstream of *let-23* in ovulation (Clandinin *et al.,* 1998). The fact that *iri-1* is, like *itr-1*, expressed in the spermatheca (Figure 3C) suggested to us that it may also function in ovulation, by modulating *itr-1* function in some way. However, when *iri-1* was knocked down only after larval stage 1, fertility was restored to wild-type levels (Figure 6E). This suggests that, either *iri-1* does not function in ovulation or it functions redundantly with an as yet unidentified gene.

The Cellular Basis of IRI-1 Function

The lack of homology to known functional domains or motifs represents a significant barrier to predicting the likely cellular functions of IRI-1 and the role that it plays in IP_3 signaling. The presence of both nuclear import and export signals perhaps suggests that it might shuttle in and out of the nucleus, which might allow it to function in the control of gene expression. Meanwhile, the presence of motifs that could bind to SH_3 domains suggests that it may function in associating ITR-1 with other proteins, a potential mechanism whereby the IP_3 receptor could be anchored to other components of a signaling pathway.

The identification of proteins that interact with the IP_3 receptor to modulate its function is beginning to elucidate the mechanisms underlying the determination and maintenance of specificity in calcium signaling pathways. Our results suggest that the interaction between ITR-1 and IRI-1 has important implications for the role of the IP_3 receptor in the control of both pharyngeal pumping rate and the defecation interval. Elucidation of the precise cellular basis of the roles of IRI-1 should therefore shed light on the mechanisms by which IP_3 signaling is responsible for the generation and modulation of biological rhythms.

ACKNOWLEDGMENTS

We are grateful to Laura Harrington for the *cnt-1::gfp* reporter strain, Robert Barstead for the yeast two-hybrid library, and Andy Fire for GFP reporter and RNAi feeding vectors. Some nematode strains used in this work were provided by the Caenorhabditis Genetics Center, which is funded by the National Institutes of Health National Center for Research Resources (NCRR).

This work was supported by the Medical Research Council (UK). H.A.B. is an MRC Senior Fellow.

REFERENCES

Avery, L., and Horvitz, H.R. (1990). Effects of starvation and neuroactive drugs on feeding in *Caenorhabditis elegans.* J. Exp. Zool. *253,* 263–270.

Baylis, H.A., Furuichi, T., Yoshikawa, F., Mikoshiba, K., and Sattelle, D.B. (1999). Inositol 1,4,5-trisphosphate receptors are strongly expressed in the nervous system, pharynx, intestine, gonad and excretory cell of *Caenorhabditis elegans* and are encoded by a single gene (*itr-1*). J. Mol. Biol. *294,* 467–476.

Berridge, M.J. (1993). Inositol trisphosphate and calcium signalling. Nature *361,* 315–325.

Berridge, M.J. (1997). Inositol trisphosphate and calcium: two interacting second messengers. Am. J. Nephrol. *17,* 1–11.

Brenner, S. (1974). The genetics of *Caenorhabditis elegans.* Genetics *77,* 71–94.

Boxem, M., and van den Heuvel, S. (2002). *C. elegans* class B synthetic multivulva genes act in G_1 regulation. Curr. Biol. *12,* 906–911.

Clandinin, T.R., DeModena, J.A., and Sternberg, P.W. (1998). Inositol trisphosphate mediates a RAS-independent response to LET-23 receptor kinase activation in *C. elegans.* Cell *92,* 523–533.

Clapham, D.E. (1995). Calcium signalling. Cell *80,* 259–268.

Clark, S.G., Lu, X., and Horvitz, H.R. (1994). The *Caenorhabditis elegans* locus *lin-15*, a negative regulator of a tyrosine kinase signalling pathway, encodes two different proteins. Genetics *137,* 987–997.

Dal Santo, P., Logan, M.A., Chisholm, A.D., and Jorgensen, E.M. (1999). The inositol trisphosphate receptor regulates a 50-second behavioral rhythm in *C. elegans.* Cell *98,* 757–767.

Eisenmann, D.M., and Kim, S.K. (2000). Protruding vulva mutants identify novel loci and wnt signalling factors that function during *Caenorhabditis elegans* vulva development. Genetics *156,* 1097–1116.

Ferguson, E.L., Sternberg, P.W., and Horvitz, H.R. (1987). A genetic pathway for the specification of the vulval cell lineages of *Caenorhabditis elegans.* Nature *326,* 259–282.

Friedman, L., Anna-Arriola, S.S., Hodgkin, J., and Kimble, J. (2000). gon-4, a cell lineage regulator required for gonadogenesis in *Caenorhabditis elegans.* Dev. Biol. *228,* 350–362.

Gower, N.J.D., Temple, G.R., Schein, J.E., Marra, M., Walker, D.S., and Baylis, H.A. (2001). Dissection of the promoter of the inositol 1,4,5-trisphosphate receptor gene, itr-1, in C. elegans: a molecular basis for cell-specific expression of IP_3R isoforms. J. Mol. Biol. *306,* 145–147.

Greenwald, I. (1997). Development of the vulva. In: *C. elegans* II, ed. D.L. Riddle, T. Blumenthal, B.J. Meyer, and J.R. Priess, Cold Spring Harbor, NY: Cold Spring Harbor Laboratory Press.

Harper, J.W., Adami, G.R., Wei, N., Keyomarsi, K., and Elledge, S.J. (1993). The p21 Cdk-interacting protein Cip1 is a potent inhibitor of G1 cyclin-dependent kinases. Cell *75,* 805–816.

Horvitz, H.R., Chalfie, M., Trent, C., Sulston, J.E., and Evans, P.D. (1982). Serotonin and octopamine in the nematode *Caenorhabditis elegans.* Science *216,* 1012–1014.

Huang, L.S., Tzou, P., and Sternberg, P.W. (1994). The *lin-15* locus encodes two negative regulators of *Caenorhabditis elegans* vulval development. Mol. Biol. Cell *5,* 395–411.

Iwasaki, K., Liu, D.W.C., and Thomas, J.H. (1995). Genes that control a temperature-compensated ultradian clock in *Caenorhabditis elegans.* Proc. Natl. Acad. Sci. USA *92,* 10317–10321.

Kay, B.K., Williamson, M.P., and Sudol, M. (2000). The importance of being proline: the interaction of proline-rich motifs in signaling proteins with their cognate domains. FASEB J. *14,* 231–241.

Kimble, J., and White, J.G. (1981). On the control of germ cell development in *Caenorhabditis elegans.* Dev. Biol. *81,* 208–219.

Kozak, M. (1986). Point mutations define a sequence flanking the AUG initiator codon that modulates translation by eukaryotic ribosomes. Cell *44,* 283–292.

Letunic, I. *et al.* (2002). Recent improvements to the SMART domain-based sequence annotation resource. Nucleic Acids Res. *30,* 242–244.

Lewis, J.A., and Fleming, J.T. (1995). Basic culture methods. Methods Cell Biol. *48,* 3–29.

Liu, D.W.C., and Thomas, J.H. (1994). Regulation of a periodic motor program in *C. elegans.* J. Neurosci. *14,* 1953–1962.

Matunis, M.J., Wu, J., and Blobel, G. (1998). SUMO-1 modification and its role in targeting the Ran GTPase-activating protein, RanGAP1, to the nuclear pore complex. J. Cell Biol. *140,* 499–509.

Mello, C., and Fire, A. (1995). DNA transformation. Methods Cell Biol. *48,* 452–482.

Miguel-Aliaga, I., Culetto, E., Walker, D.S., Baylis, H.A., Sattelle, D.B., and Davies, K.E. (1999). The *Caenorhabditis elegans* orthologue responsible for spinal muscular atrophy is a maternal product critical for germline maturation and embryonic viability. Hum. Mol. Genet. *8,* 2133–2143.

Miskowski, J., Li, Y., and Kimble, J. (2001). The *sys-1* gene and sexual dimorphism during gonadogenesis in *Caenorhabditis elegans.* Dev. Biol. *230,* 61–73.

Nakai, K., and Horton, P. (1999). PSORT: a program for detecting sorting signals in proteins and predicting their subcellular localization. Trends Biochem. Sci. *24,* 34–36.

Niacaris, T., and Avery, L. (2003). Serotonin regulates repolarization of the *C. elegans* pharyngeal muscle. J. Exp. Biol. *206,* 223–231.

Nishimoto, T. (2000). Upstream and downstream of ran GTPase. Biol. Chem. *381,* 397–405.

Patel, S. Joseph, S.K., and Thomas, A.P. (1999). Molecular properties of inositol 1,4,5-trisphosphate receptors. Cell Calcium *25,* 247–264.

Quaroni, A., and Paul, E.C.A. (1999). Cytocentrin is a Ral-binding protein involved in the assembly and function of the mitotic apparatus. J. Cell Sci. *112,* 707–718.

Ridley, A.J. (1995). Rho-related proteins: actin cytoskeleton and cell cycle. Curr. Opin. Genet. Dev. *5,* 24–30.

Schultz, J., Milpetz, F., Bork, P., and Ponting, C.P. (1998). SMART, a simple modular architecture research tool: Identification of signaling domains. Proc. Natl. Acad. Sci. USA *95,* 5857–5864.

Seydoux, G., Savage, C., and Greenwald, I. (1993). Isolation and characterisation of mutations causing abnormal eversion of the vulva in *Caenorhabditis elegans.* Dev. Biol. *157,* 423–436.

Siegfried, K.R., and Kimble, J. (2002). POP-1 controls axis formation during early gonadogenesis in *C. elegans.* Development *129,* 443–453.

Takeuchi, M., Kawakami, M., Ishihara, T., Amano, T., Kondo, K., and Katsura, I. (1998). An ion channel of the degenerin/epithelial sodium channel superfamily controls the defecation rhythm in *Caenorhabditis elegans.* Proc. Natl. Acad. Sci. USA *95,* 11775–11780.

Taylor, C.W., Genazzani, A.A., and Morris, S.A. (1999). Expression of inositol trisphosphate receptors. Cell Calcium *26,* 237–251.

Timmons, L., Court, D.L., and Fire, A. (2001). Ingestion of bacterially expressed dsRNAs can produce specific and potent genetic interference in *Caenorhabditis elegans.* Gene *263,* 103–112.

Walker, D., Bichet, D., Campbell, K.P., and De Waard, M. (1998). A β_4 isoform-specific interaction site in the carboxyl-terminal region of the voltage-dependent Ca^{2+} channel α_1A subunit. J. Biol. Chem. *273,* 2361–2367.

Walker, D.S., Gower, N.J.D., Ly, S., Bradley, G.L., and Baylis, H.A. (2002a). Regulated disruption of inositol 1,4,5-trisphosphate (IP_3) signaling in *C. elegans* reveals new functions in feeding and embryogenesis. Mol. Biol. Cell *13,* 1329–1337.

Walker, D.S., Ly, S., Lockwood, K.C., and Baylis, H.A. (2002b). A direct interaction between IP_3 receptors and myosin II regulates IP_3 signalling in *C. elegans.* Curr. Biol. *12,* 951–956.